Lawrence Berkeley National Laboratory

Title
Exact seismic velocities for VTI and HTI media and extended Thomsen Formulas for stronger

anisotropies

Permalink
https://escholarship.org/uc/item/96t6g3vw

Author
Berryman, J.G.

Publication Date
2008-06-24

Peer reviewed

Exact Seismic Velocities for VTI and HTI Media and Extended Thomsen Formulas for Stronger Anisotropies

James G. Berryman[1,*]

[1]*University of California, Lawrence Berkeley National Laboratory,*

1 Cyclotron Road, MS 90R1116, Berkeley, CA 94720, USA

Abstract

I explore a different type of approximation to the exact anisotropic wave velocities as a function of incidence angle in vertically transversely isotropic (VTI) media. This method extends the Thomsen weak anisotropy approach to stronger anisotropy without significantly affecting the simplicity of the formulas. One important improvement is that the peak of the quasi-SV-wave speed $v_{sv}(\theta)$ is located at the correct incidence angle $\theta = \theta_{max}$, rather than always being at the position $\theta = 45^o$, which universally holds for Thomsen's approximation — although $\theta_{max} = 45^o$ is actually never correct for any VTI anisotropic medium. The magnitudes of all the wave speeds are also more closely approximated for all values of the incidence angle. Furthermore, the value of θ_{max} (which is needed in the new formulas) can be deduced from the same data that are typically used in the weak anisotropy data analysis. The two examples presented are based on systems having vertical fractures. The first set of model fractures has their axes of symmetry randomly oriented in the horizontal plane. Such a system is then isotropic in the horizontal plane and, therefore, exhibits vertical transverse isotropic (VTI) symmetry. The second set of fractures also has axes of symmetry in the horizontal plane, but it is assumed these axes are aligned so that the system exhibits horizontal transverse isotropic (HTI) symmetry. Both types of systems are easily treated with the new wave speed formulation.

---

[*]`JGBerryman@LBL.GOV`

INTRODUCTION

Thomsen's weak anisotropy method (Thomsen, 1986) was originally formulated for media having vertical transversely isotropic (VTI) symmetry. This method is independent of the mechanism of nature producing the anisotropy, whether it be due to layering, or horizontal fractures, or randomly oriented vertical fractures, or some other source. So the method has wide applicability for use in exploration problems. However, when the results of the original formulation are compared to exact results for the same VTI media, it is easy to see that there are some deficiencies. In particular, the vertically polarized (SV) shear wave will always have a peak (or possibly a trough) somewhere in the range $0 \leq \theta \leq \pi/2 = 90^o$. Thomsen's weak anisotropy formulation always puts this extreme point exactly at $\theta_m = \pi/2 = 45^o$. However, this location of θ_m never occurs for any interesting degree of VTI anisotropy, although it may be close to the truth for extremely weak anisotropy (very low horizontal crack density is one example of this). In an effort to determine whether it was possible to improve on this approximation, I have found that a relatively small modification of Thomsen's formulas places the extreme v_{sv} point at the right location θ_m, and also improves the fit of both $v_{sv}(\theta)$ and $v_p(\theta)$ to the exact VTI curves. The ultimate cost of this improvement is negligible since the data required to estimate the location of θ_m are exactly the same as the data used to determine Thomsen's other parameters for weak anisotropy. The method can also be used with only minor modifications for media have horizontal transversely isotropic (HTI) symmetry, such as reservoirs having aligned vertical fractures. The paper focuses on the general theory and uses other recent work relating fracture influence parameters (Sayers and Kachanov, 1991; Berryman and Grechka, 2006) to provide some useful examples of the applicability of the new method.

The next section reviews the standard results for wave speeds in a VTI medium, and also presents the Thomsen weak anisotropy results. The following section presents the analysis leading to the extended anisotropy method, that allows the wave speed formulas to reflect more accurately the correct behavior near the extremes (greatest excursions from the values at normal incidence and near horizontal incidence). The next section shows how to determine the value of θ_m (the incidence angle at which the extreme SV-wave behavior occurs) from the same data already used in Thomsen's formulas. Then, normal moveout corrections are recomputed for the new formulation, and it is found that the results are identical to those for

Thomsen formulation; thus, no new corrections are needed near normal incidence. Finally, models of VTI and HTI reservoirs having vertical fractures are computed using the new wave speed formulation and compared to prior results. Appendix A computes the quasi-SV-wave speed at $\theta = \theta_m$, exactly and at two levels of approximation in order to have values to check against the results in the main text. Appendix B collects some trigonometric identities needed in the main text. Appendix C discusses how to get HTI results simply and directly from VTI results, both for the exact wave speeds and for the new approximate wave speed formulas.

THOMSEN'S WEAK ANISOTROPY METHOD FOR SEISMIC WAVES

Thomsen's weak anisotropy method (Thomsen, 1986), being an approximation designed specifically for use in velocity analysis for exploration geophysics, is clearly not exact. Approximations incorporated into the formulas become most apparent for angles θ greater than about 15° from the vertical, especially for compressional and vertically polarized shear wave velocities $v_p(\theta)$ and $v_{sv}(\theta)$, respectively. Angle θ is measured from the $\hat{z}$-vector pointing into the earth.

For reference purposes, we include here the exact velocity formulas for P, SV, and SH seismic waves at all angles in a VTI elastic medium. These results are available in many places (Rüger, 2002; Thomsen, 2002; Musgrave, 1959, 2003), but were taken specifically from Berryman (1979) with some minor changes of notation. The results are:

$$v_p^2(\theta) = \frac{1}{2\rho} \left\{ \left[(c_{11} + c_{44}) \sin^2 \theta + (c_{33} + c_{44}) \cos^2 \theta \right] + R(\theta) \right\} \tag{1}$$

and

$$v_{sv}^2(\theta) = \frac{1}{2\rho} \left\{ \left[(c_{11} + c_{44}) \sin^2 \theta + (c_{33} + c_{44}) \cos^2 \theta \right] - R(\theta) \right\}, \tag{2}$$

where

$$R(\theta) = \sqrt{ \left[(c_{11} - c_{44}) \sin^2 \theta - (c_{33} - c_{44}) \cos^2 \theta \right]^2 + 4 \left(c_{13} + c_{44} \right)^2 \sin^2 \theta \cos^2 \theta } \tag{3}$$

and, finally,

$$v_{sh}^2(\theta) = \frac{1}{\rho} \left[c_{44} + (c_{66} - c_{44}) \sin^2 \theta \right]. \tag{4}$$

3

The stiffness matrix c_{ij} is defined for $i, j = 1, \ldots, 6$ by

$$c_{ij} = \begin{pmatrix} c_{11} & c_{12} & c_{13} & & & \\ c_{12} & c_{11} & c_{13} & & & \\ c_{13} & c_{13} & c_{33} & & & \\ & & & c_{44} & & \\ & & & & c_{44} & \\ & & & & & c_{66} \end{pmatrix}, \tag{5}$$

where — for VTI symmetry – $c_{12} = c_{11} - 2c_{66}$. In an isotropic system (which is a more restrictive case than our current interests), $c_{12} = c_{13} = \lambda$, $c_{44} = c_{66} = \mu$, and $c_{11} = c_{33} = \lambda + 2\mu$, where λ and μ are the usual Lamé constants. The definition (5) makes use of the Voigt notation, (*i.e.,* 6×6 matrix instead of 4th order tensor), and relates stress σ_{ij} to strain ϵ_{ij} via $\sigma_{ij} = \Sigma_k c_{ik}\epsilon_{kj}$. For VTI symmetry, we take $x_3 = z$ (the vertical) as the axis of symmetry. But, for HTI symmetry, we may choose x_3 to be some other direction (such as horizontal directions x or y, or some linear combination).

Expressions for phase velocities in Thomsen's weak anisotropy limit can be found in many places, including Thomsen (1986, 2002) and Rüger (2002). The pertinent expressions for phase velocities in VTI media as a function of angle θ, measured as previously mentioned from the vertical direction, are

$$v_p(\theta) \simeq v_p(0) \left(1 + \epsilon \sin^2 \theta - (\epsilon - \delta) \sin^2 \theta \cos^2 \theta\right), \tag{6}$$

$$v_{sv}(\theta) \simeq v_s(0) \left(1 + [v_p^2(0)/v_s^2(0)] (\epsilon - \delta) \sin^2 \theta \cos^2 \theta\right), \tag{7}$$

and

$$v_{sh}(\theta) \simeq v_s(0) \left(1 + \gamma \sin^2 \theta\right). \tag{8}$$

In our present context, $v_s(0) = \sqrt{c_{44}/\rho_0}$, and $v_p(0) = \sqrt{c_{33}/\rho_0}$, where c_{33}, c_{44}, and ρ_0 are two stiffnesses of the cracked medium and the mass density of the isotropic host elastic medium. We assume that the cracks have insufficient volume to affect the mass density significantly. The three Thomsen (1986) seismic parameters appearing in (6)–(8) for weak anisotropy with VTI symmetry are $\gamma = (c_{66} - c_{44})/2c_{44}$, $\epsilon = (c_{11} - c_{33})/2c_{33}$, and

$$\delta = \frac{(c_{13} + c_{44})^2 - (c_{33} - c_{44})^2}{2c_{33}(c_{33} - c_{44})} = \left(\frac{c_{33} + c_{13}}{2c_{33}}\right)\left(\frac{c_{13} + 2c_{44} - c_{33}}{c_{33} - c_{44}}\right). \tag{9}$$

All three of these parameters can play important roles in the velocities given by (6)-(8) when the crack densities are high enough. If crack densities are very low, then the SV shear wave will actually have no dependence on angle of wave propagation. Note that the so-called anellipticity parameter, $A = \epsilon - \delta$, vanishes when $\epsilon \equiv \delta$ — which we will see does happen for low crack densities.

For each of these velocities, the derivation of Thomsen's approximation has included a step that removes the square on the left-hand side of the equation, by expanding a square root of the right hand side. This step introduces a factor of $\frac{1}{2}$ multiplying the $\sin^2 \theta$ terms on the right hand side, and — for example — immediately explains how equation (8) is obtained from (4). The other two equations for $v_p(\theta)$ and $v_{sv}(\theta)$, *i.e.*, (6) & (7), involve additional approximations. More details about the nature of these approximations follow.

EXTENDED APPROXIMATIONS FOR ANISOTROPIC WAVE SPEEDS

The biggest and most obvious problem with Thomsen's approximations to the wave speeds generally occurs in $v_{sv}(\theta)$. The key issue is that Thomsen's approximation for $v_{sv}(\theta)$ is completely symmetric around $\theta = \pi/4 = 45^o$, while this is generally not true of the actual wave speeds $v_{sv}(\theta)$. This error may seem innocuous in itself, but it also can lead to large over or under estimates of wave speeds in the neighborhood of $\theta = 45^o$. To correct this problem while still making use of a practical approximation to the wave speed, we reconsider an approach originally proposed by Berryman (1979). In particular, notice that the square root formula for $R(\theta)$ can be conveniently, and exactly, rewritten as:

$$R(\theta) = [(c_{11} - c_{44}) \sin^2 \theta + (c_{33} - c_{44}) \cos^2 \theta] \sqrt{1 - \zeta(\theta)}, \tag{10}$$

where

$$\zeta(\theta) \equiv 4 \frac{[(c_{11} - c_{44})(c_{33} - c_{44}) - (c_{13} + c_{44})^2] \sin^2 \theta \cos^2 \theta}{[(c_{11} - c_{44}) \sin^2 \theta + (c_{33} - c_{44}) \cos^2 \theta]^2}. \tag{11}$$

To simplify this expression, first notice that ζ has an absolute maximum value, which occurs when θ takes the value θ_m determined by

$$\tan^2 \theta_m = \frac{c_{33} - c_{44}}{c_{11} - c_{44}}. \tag{12}$$

This maximum value of ζ is given by

$$\zeta_m = 1 - \frac{(c_{13} + c_{44})^2}{(c_{11} - c_{44})(c_{33} - c_{44})} = (\epsilon - \delta) \frac{2c_{33}}{c_{11} - c_{44}}, \tag{13}$$

5

where the second expression relates ζ_m to the difference between the Thomsen parameters ϵ and δ. Then, $\zeta(\theta)$ can be rewritten as

$$\zeta(\theta) = \frac{2\zeta_m}{1 + \chi(\theta)}, \tag{14}$$

where

$$\chi(\theta) = \frac{1}{2} \left[\frac{\tan^2 \theta}{\tan^2 \theta_m} + \frac{\tan^2 \theta_m}{\tan^2 \theta} \right]. \tag{15}$$

An alternative expression for $\chi(\theta)$ is given by

$$\chi(\theta) \equiv \cosh a(\theta), \tag{16}$$

where

$$a(\theta) = \ln \left[\frac{c_{11} - c_{44}}{c_{33} - c_{44}} \tan^2 \theta \right] = \ln \left[\frac{\tan^2 \theta}{\tan^2 \theta_m} \right]. \tag{17}$$

For realistic systems, it is always true that $0 \le \zeta(\theta) \le 1$. So, we can expand the square root in (10), keeping just its first order Taylor series correction, which is

$$\sqrt{1 - \zeta(\theta)} \simeq 1 - \frac{\zeta(\theta)}{2} = 1 - \frac{\zeta_m}{1 + \chi(\theta)}. \tag{18}$$

Results for $v_p(\theta)$ and $v_{sv}(\theta)$ then become:

$$v_p^2(\theta) \simeq \frac{1}{\rho} \left\{ \left[c_{11} \sin^2 \theta + c_{33} \cos^2 \theta \right] - \frac{\zeta_m[(c_{11} - c_{44}) \sin^2 \theta + (c_{33} - c_{44}) \cos^2 \theta]}{2[1 + \chi(\theta)]} \right\} \tag{19}$$

and

$$v_{sv}^2(\theta) \simeq \frac{1}{\rho} \left\{ c_{44} + \frac{\zeta_m[(c_{11} - c_{44}) \sin^2 \theta + (c_{33} - c_{44}) \cos^2 \theta]}{2[1 + \chi(\theta)]} \right\}. \tag{20}$$

Note that the only approximation made in arriving at (19) and (20) was the approximation of the square root in (18).

Further progress can be made by first noting that the quantity $1 + \chi(\theta)$ may be written as a perfect square:

$$1 + \chi(\theta) = \left[\frac{1}{\sqrt{2}} \left(\frac{\tan \theta}{\tan \theta_m} + \frac{\tan \theta_m}{\tan \theta} \right) \right]^2. \tag{21}$$

This expression is simplified using trigonometric identities in Appendix B.

Making use of (55), our final result for $\zeta(\theta)$ is

$$\zeta(\theta) = \frac{\zeta_m \sin^2 2\theta_m \sin^2 2\theta}{[1 - \cos 2\theta_m \cos 2\theta]^2}. \tag{22}$$

Note that no approximations were made in arriving at (22). [Remark: The only approximations made to the wave speeds in this paper involve Taylor expansions of square roots.]

6

Combining (22) with definition (11), we also can show that

$$[(c_{11} - c_{44}) \sin^2 \theta + (c_{33} - c_{44}) \cos^2 \theta]^2 = (c_{11} - c_{44})(c_{33} - c_{44}) \frac{4\zeta_m \sin^2 \theta \cos^2 \theta}{\zeta(\theta)}$$

$$= (c_{11} - c_{44})(c_{33} - c_{44}) \frac{[1 - \cos 2\theta_m \cos 2\theta]^2}{\sin^2 2\theta_m}$$

$$= (c_{11} - c_{44})^2 \tan^2 \theta_m \frac{[1 - \cos 2\theta_m \cos 2\theta]^2}{4 \sin^2 \theta_m \cos^2 \theta_m}$$

$$= (c_{11} - c_{44})^2 \frac{[1 - \cos 2\theta_m \cos 2\theta]^2}{4 \cos^4 \theta_m}.$$

So it follows that

$$\sin^2 \theta + \tan^2 \theta_m \cos^2 \theta = \frac{[1 - \cos 2\theta_m \cos 2\theta]}{2 \cos^2 \theta_m}, \tag{23}$$

which is another useful identity that can be checked directly.

Then, making use of the identity $\sin^2 2\theta_m / \cos^2 \theta_m = 4 \sin^2 \theta_m$, the speed of the SV-wave is given by

$$\rho v_{sv}^2(\theta) \simeq c_{44} + (c_{11} - c_{44})\zeta_m \frac{2 \sin^2 \theta_m \sin^2 \theta \cos^2 \theta}{[1 - \cos 2\theta_m \cos 2\theta]}. \tag{24}$$

Similarly, the speed of the P-wave is given by

$$\rho v_p^2 \simeq c_{33} + (c_{11} - c_{33}) \sin^2 \theta - (c_{11} - c_{44})\zeta_m \frac{2 \sin^2 \theta_m \sin^2 \theta \cos^2 \theta}{[1 - \cos 2\theta_m \cos 2\theta]}. \tag{25}$$

Again, the only approximation made in these two expressions is the one due to expanding the square root in (18).

A more direct comparison with Thomsen's approximations uses (24) and (25) to arrive at approximate formulas for $v_{sv}(\theta)$ and $v_p(\theta)$ analogous to Thomsen's. The resulting expressions are

$$v_p(\theta)/v_p(0) \simeq 1 + \epsilon \sin^2 \theta - (\epsilon - \delta) \frac{2 \sin^2 \theta_m \sin^2 \theta \cos^2 \theta}{[1 - \cos 2\theta_m \cos 2\theta]} \tag{26}$$

and

$$v_{sv}(\theta)/v_s(0) \simeq 1 + \left[v_p^2(0)/v_s^2(0)\right] (\epsilon - \delta) \frac{2 \sin^2 \theta_m \sin^2 \theta \cos^2 \theta}{[1 - \cos 2\theta_m \cos 2\theta]}. \tag{27}$$

Equations (26) and (27) are the two main results of this paper. So far only two approximations have been made, and these both came from expanding a square root in a Taylor series, and retaining only the first nontrivial term.

Comparing (26) and (27) to (6) and (7), the differences are found to lie in a factor of the form:

$$\frac{2 \sin^2 \theta_m}{[1 - \cos 2\theta_m \cos 2\theta]} \rightarrow \frac{1}{2 \cos^2 \theta_m} \qquad \text{as} \qquad \theta \rightarrow \theta_m, \tag{28}$$

which depends explicitly on the angle θ_m determined by $\tan^2 \theta_m = (c_{33} - c_{44})/(c_{11} - c_{44})$, and also on θ itself. As indicated, the expression goes to $1/2 \cos^2 \theta_m$ in the limit of $\theta \to \theta_m$, which is also in agreement with the results for $v_{sv}(\theta_m)$ in Appendix A. But, since $\sin^2 \theta_m = \tan^2 \theta_m/(1 + \tan^2 \theta_m)$ and $\cos 2\theta_m = (1 - \tan^2 \theta_m)/(1 + \tan^2 \theta_m)$, useful identities are

$$\sin^2 \theta_m = \frac{c_{33} - c_{44}}{c_{11} + c_{33} - 2c_{44}} = 1 - \cos^2 \theta_m \tag{29}$$

and

$$\cos 2\theta_m = \frac{c_{11} - c_{33}}{c_{11} + c_{33} - 2c_{44}} = 1 - 2\sin^2 \theta_m. \tag{30}$$

These results can therefore be used, after deducing some of the elastic constants from our data at near offsets, in order to extend the validity of the equations to greater angles and farther offsets. Inversion of such data is however beyond the paper's scope.

To make these formulas (26) and (27) look as much as possible like Thomsen's formulas — and thereby arrive at a somewhat different understanding of equations (6) and (7), eliminate θ_m by arbitrarily setting it equal to some value such as $\theta_m = 45^o$, in which case $2\sin^2 \theta_m = 1$ and $\cos 2\theta_m = 0$. Then, the θ dependence in the denominators goes away, and Thomsen's formulas (6) and (7) are recovered exactly. This choice of $\theta_m = 45^o$ is however completely unnecessary as shall be shown, and furthermore is never valid for any anisotropic medium with $c_{11} \neq c_{33}$.

DEDUCING θ_m FROM SEISMIC DATA

The key quantity needed in the extended formulas for seismic data is clearly the value of the angle θ_m. However, this value is quite easily determined because

$$\tan^2 \theta_m = \frac{c_{33} - c_{44}}{c_{11} - c_{44}} = \frac{v_p^2(0) - v_s^2(0)}{c_{11}/\rho - v_s^2(0)} \tag{31}$$

and

$$\epsilon = \frac{c_{11} - c_{33}}{2c_{33}} = \frac{c_{11}/\rho - v_p^2(0)}{2v_p^2(0)}. \tag{32}$$

Therefore,

$$\tan^2 \theta_m = \frac{v_p^2(0) - v_s^2(0)}{(1 + 2\epsilon)v_p^2(0) - v_s^2(0)}. \tag{33}$$

Thus, θ_m is completely determined by the same data used in the standard analysis of reflection seismic data that determines the various small angle wave speeds and the Thomsen parameters.

8

The pertinent factors for use in the formulas are given by

$$\sin^2 \theta_m = \frac{v_p^2(0) - v_s^2(0)}{2[(1 + \epsilon)v_p^2(0) - v_s^2(0)]} \tag{34}$$

and

$$\cos 2\theta_m = \frac{\epsilon v_p^2(0)}{(1 + \epsilon)v_p^2(0) - v_s^2(0)}. \tag{35}$$

NORMAL MOVEOUT CORRECTIONS

The altered forms of $v_p(\theta)$ and $v_{sv}(\theta)$ in equations (26) and (27) suggest that it might also be necessary to alter the normal moveout corrections to the velocities (Tsvankin, 2005, p. 113). It is easy to see that these corrections are now given by

$$V_{NMO,p} = v_p(0)\sqrt{1 + 2\delta}, \tag{36}$$

for the quasi-P-wave, and,

$$V_{NMO,sv} = v_s(0)\sqrt{1 + 2\sigma}, \tag{37}$$

for the quasi-SV-wave, where

$$\sigma = \left[v_p^2(0)/v_s^2(0)\right](\epsilon - \delta). \tag{38}$$

These corrections to the NMO velocities are exactly the same as those for Thomsen's weak anisotropy approximation because the factor that is pertinent, and that has potential to alter these expressions is given, in the small angle limit $\theta \to 0$, by

$$\frac{2\sin^2 \theta_m}{1 - \cos 2\theta_m} \equiv 1. \tag{39}$$

Since Thomsen's formulas accurately approximate all three wave speeds in this limit by design, the present formulas share this accuracy (and in some cases improves upon it). Therefore, no changes are needed in short offset (small θ) data processing. The NMO correction for the SH-wave clearly does not change either.

RESERVOIRS WITH VERTICALLY ORIENTED FRACTURES

To provide some pertinent examples of results for the types of anisotropic media most interesting in oil and gas reservoirs, two distinct types of reservoirs having vertical fractures

will be considered. The first case considered will have vertical fractures that are not preferentially aligned, so the reservoir symmetry is vertical transverse isotropy (VTI). The second case will also have vertical fractures but these will be preferentially aligned, so the reservoir symmetry will be horizontal transverse isotropy and, therefore, exhibit azimuthal (angle ϕ dependent) anisotropy.

These two reservoir fracture models will be built up using results from recent numerical experiments by Grechka and Kachanov (2006a,b). Those results were analyzed by Berryman and Grechka (2006) in light of the crack influence parameter formalism of Kachanov (1980) and Sayers and Kachanov (1991). The significance of these crack influence parameters for the case of aligned horizontal cracks for lower crack densities $\rho_c = na^3$ (where $n = N/V$ is the number density of cracks and for penny-shaped cracks a is the radius of the penny while b/a is the aspect ratio) is:

$$\Delta S_{ij}^{(1H)} = \rho_c \begin{pmatrix} 0 & 0 & \eta_1 & & & \\ 0 & 0 & \eta_1 & & & \\ \eta_1 & \eta_1 & 2(\eta_1 + \eta_2) & & & \\ & & & 2\eta_2 & & \\ & & & & 2\eta_2 & \\ & & & & & 0 \end{pmatrix}. \tag{40}$$

Typical values of crack density ρ_c for reserviors are $\rho_c \leq 0.1$. The matrix $\Delta S_{ij}^{(1H)}$ is the lowest order compliance correction matrix and should be added to the isotropic compliance matrix

$$\Delta S_{ij}^{(0)} = \begin{pmatrix} 1/E & -\nu/E & -\nu/E & & & \\ -\nu/E & 1/E & -\nu/E & & & \\ -\nu/E & -\nu/E & 1/E & & & \\ & & & 1/G & & \\ & & & & 1/G & \\ & & & & & 1/G \end{pmatrix}, \tag{41}$$

where $\nu = \lambda/2(\lambda + \mu)$ is Poisson's ratio, $G = \mu$ is the shear modulus, and $E = 2(1 + \nu)G$ is Young's modulus of the (assumed) isotropic background medium. Summing (41) and (40) produces the compliance matrix for a horizontally cracked, VTI elastic medium. We can use this combined matrix to compute the behavior of a simple HTI reservoir with aligned vertical cracks using the methods described in Appendix C.

For vertical fractures with randomly oriented axes of symmetry, the resulting VTI medium has a low crack density correction matrix of the form

$$\Delta S_{ij}^{(1V)} = \rho_c \begin{pmatrix} (\eta_1 + \eta_2) & \eta_1 & \eta_1/2 & & & \\ \eta_1 & (\eta_1 + \eta_2) & \eta_1/2 & & & \\ \eta_1/2 & \eta_1/2 & 0 & & & \\ & & & \eta_2 & & \\ & & & & \eta_2 & \\ & & & & & 2\eta_2 \end{pmatrix}, \tag{42}$$

in which the η's have the same values as those in (40) if the only difference between the cracks in (42) and (40) is their orientation. Note that $2\Delta S_{ij}^{(1V)} + \Delta S_{ij}^{(1H)}$ is an isotropic correction matrix for a system having crack density $3\rho_c$. Summing (41) and (42) produces the compliance matrix for a vertically cracked VTI elastic medium, in which the crack normals are randomly and/or uniformly distributed in the horizontal plane.

Higher order corrections (*i.e.*, second order in powers of ρ_c) in the Sayers and Kachanov (1991) formulation take the form:

$$\Delta S_{ij}^{(2H)} = \rho_c^2 \begin{pmatrix} 0 & 0 & \eta_4 & & & \\ 0 & 0 & \eta_4 & & & \\ \eta_4 & \eta_4 & 2(\eta_3 + \eta_4 + \eta_5) & & & \\ & & & 2\eta_5 & & \\ & & & & 2\eta_5 & \\ & & & & & 0 \end{pmatrix} \tag{43}$$

for horizontal fractures — *i.e.*, to be combined with (40). Similarly,

$$\Delta S_{ij}^{(2V)} = \rho_c^2 \begin{pmatrix} (\eta_3 + \eta_4 + \eta_5) & \eta_4 & \eta_4/2 & & & \\ \eta_4 & (\eta_3 + \eta_4 + \eta_5) & \eta_4/2 & & & \\ \eta_4/2 & \eta_4/2 & 0 & & & \\ & & & \eta_5 & & \\ & & & & \eta_5 & \\ & & & & & 2(\eta_3 + \eta_5) \end{pmatrix} \tag{44}$$

for the random vertical fractures producing VTI symmetry – to be combined with (42)

Examples of values of all five of these crack influence parameters have been obtained based on the numerical studies of Grechka and Kachanov (2006a,b) by Berryman and Grechka

11

(2006). The two models considered have very different Poisson's ratios for the isotropic background media: (1) $\nu_0 = 0.00$ and (2) $\nu_0 = 0.4375$. We will call these two models, respectively, the first model and the second model. The first model has background stiffness matrix values $c_{11} = c_{22} = c_{33} = 13.75$ GPa, $c_{12} = c_{13} = c_{23} = 0.00$ GPa, and $c_{44} = c_{55} = c_{66} = 6.875$ GPa. Bulk modulus for this model is therefore $K_0 = 4.583$ GPa and shear modulus is $G_0 = 6.875$ GPa. The second model has stiffness matrix values $c_{11} = c_{22} = c_{33} = 19.80$ GPa, $c_{12} = c_{13} = c_{23} = 15.40$ GPa, and $c_{44} = c_{55} = c_{66} = 2.20$ GPa. Bulk modulus for this model is therefore $K_0 = 16.86$ GPa and shear modulus is $G_0 = 2.20$ GPa. The second model also corresponds to a background material having compressional wave speed $V_p = 3$ km/s, shear wave speed $V_s = 1$ km/s, and mass density $\rho_m = 2200.0$ kg/m^3. Detailed discussion of the method used to obtain the crack influence parameters is given by Berryman and Grechka (2006), and will not be repeated here. Results are listed in Table 1.

In all the following plots, the exact curves (as computed for the model c_{ij}'s) are plotted first in black, then the Thomsen approximation is plotted in red, and finally the new approximation is plotted in blue. Thus, in those examples where red curves appear to be missing, this happens because the blue curves lie right on top of the red ones (to graphical accuracy). This overlay effect is expected whenever θ_m approaches 45°, which can happen at low crack densities since the background medium has been taken to be isotropic.

VTI Symmetry

Figure 1 presents results for the case of vertical fractures having an isotropic distribution of normals (symmetry axes) in the horizontal plane. The resulting medium has VTI symmetry.

A first observation is that the low crack density results for $v_{sv}(\theta)$ are nearly constant, showing that $\epsilon - \delta \simeq 0$. When this happens for $v_{sv}(\theta)$, it is also true that $v_p(\theta)$ is approximately elliptical. Of course, the exact results for $v_{sh}(\theta)$ are always elliptical, but the Thomsen and new approximate results are only approximately elliptical.

Secondly, all three velocity models (exact, Thomsen, and new) give very similar results for all cases shown when $\nu_0 = 0.4375$. There are however some significant differences among the results for $\nu_0 = 0.00$, especially for $v_{sv}(\theta)$ and $v_p(\theta)$ – the largest deviations from the exact curves being those for Thomsen's approximatiosn (red curves) in both cases.

HTI Symmetry

Figure 2 presents results for vertical fractures having their normals (axes of symmetry) aligned in some direction (say $x_3 = x$). The fracture models considered are the same and use the same data as for the preceding (VTI) case.

Thomsen's approximation and the new one are virtually identical here in $v_{sh}(\theta)$ for both $\nu_0 = 0.00$ and $\nu_0 = 0.4375$. For $v_{sv}(\theta)$, Thomsen's approximation is higher than the exact result, while the new approximation is lower.

Results for $v_p(\theta)$ in both Thomsen's and the new approximation are comparable to the exact results for θ's up to about 45°–50°, but are not identical to each other or to the exact result. For $\nu_0 = 0.4375$, agreement among the three curves is good for $v_p(\theta)$, but not so good for $v_{sv}(\theta)$ or $v_{sh}(\theta)$.

SUMMARY AND CONCLUSIONS

The main results of the paper are summarized in equations (26) and (27). These formulas generalize (*i.e.*, extend the validity of) Thomsen's weak anisotropy to wider ranges of angles, and stronger anisotropy. These formulas have the clear advantage that they require no more data analysis than Thomsen's formulas for weak anisotropy, but they give more accurate predictions of the wave speeds for longer offsets. In particular, the new formulas are designed to give the peak (or possibly the trough) of the quasi-SV-wave in the right location, (*i.e.*, the correct angle $\theta = \theta_m$ with the vertical), even though the magnitude of these velocities may still be a bit off. This error made in the velocity magnitude is always less than that made using the original Thomsen formulas. Furthermore, the only new parameter needed for implementation is the angle θ_m; but this value can also be determined from the same data required to compute all the Thomsen parameters. A final advantage that is especially helpful for the practical use of the method is that the corrections needed for all the NMO velocities do not change, and so are exactly the same as for Thomsen's method.

The work presented here has necessarily been restricted to VTI and HTI symmetries, because these are the cases that correspond to the simplest and most studied cases in the anisotropy literature. It has been noted, however, that the HTI symmetry in particular is actually a fairly unrealistic model for seismic exploration problems (Tsvankin, 1997; Thom-

sen, 2002; Tsvankin, 2005). The reason for this is that the earth, to a first approximation, is often horizontally layered and such horizontal layering is well-known to produce VTI symmetry (Backus, 1962). If aligned vertical fractures are added to this already anisotropic background medium (unlike the isotropic background medium used in the present models), then the resulting symmetry is likely to be closer to orthorhombic than to HTI. This viewpoint no doubt provides a valid criticism of the work presented here. But the author does not expect this paper to be the last one on this topic, and future efforts will surely be devoted to obtaining comparable results for these more realistic cases.

APPENDIX A: $v_{sv}(\theta_m)$

For purposes of comparison, it is useful to know the exact value and also some related approximations to the exact value of the quasi-SV wave speed $v_{sv}(\theta)$ at its extreme value when $\theta = \theta_m$.

Evaluation gives the exact result

$$v_{sv}^2(\theta_m) = \frac{\sin^2 \theta_m}{2\rho}(c_{11} - c_{44}) \left[\frac{c_{11} + c_{44}}{c_{11} - c_{44}} + \frac{c_{33} + c_{44}}{c_{33} - c_{44}} - 2\sqrt{1 - \zeta_m} \right]. \tag{45}$$

After substituting $\sin^2 \theta_m = (c_{33} - c_{44})/(c_{11} + c_{33} - 2c_{44})$, expanding the square root $\sqrt{1 - \zeta_m} \simeq 1 - \zeta_m/2$, and several more steps of simplification, a useful approximate expression is

$$v_{sv}^2(\theta_m) \simeq v_s^2(0) \left[1 + \frac{\zeta_m}{2} \frac{(c_{11} - c_{44})(c_{33} - c_{44})}{c_{44}(c_{11} + c_{33} - 2c_{44})} \right]. \tag{46}$$

And finally, by approximating the square root of this expression and using (13), we have

$$\frac{v_{sv}(\theta_m)}{v_s(0)} \simeq 1 + \frac{\zeta_m(c_{11} - c_{44}) \sin^2 \theta_m}{4c_{44}} = 1 + [v_p^2(0)/v_s^2(0)] (\epsilon - \delta) \frac{\sin^2 \theta_m}{2}. \tag{47}$$

Equation (47) can be directly compared to Thomsen's formula (7). The only difference is a factor of $2\cos^2\theta_m$ in the final term. This factor could be unity if $\theta_m = 45^o$, but — since this never happens for anisotropic media — the factor always differs from unity and can be either higher or lower than unity depending on whether θ_m is less than or greater than 45°.

APPENDIX B: Some Useful Trigonometric Relations

The following calculation is needed to evaluate $\zeta(\theta)$ using (21).

It is not difficult to show (the easiest way to do this is first to reexpress the tangents using complex exponentials and then rearrange terms) that

$$\left(\frac{\tan\theta}{\tan\theta_m} + \frac{\tan\theta_m}{\tan\theta}\right) = 2\left[\frac{\sin^2(\theta+\theta_m) + \sin^2(\theta-\theta_m)}{\sin^2(\theta+\theta_m) - \sin^2(\theta-\theta_m)}\right]. \tag{48}$$

The denominator of the right hand side of this expression can be rewritten as

$$[\sin(\theta+\theta_m) + \sin(\theta-\theta_m)][\sin(\theta_m+\theta) + \sin(\theta_m-\theta)] = 4\sin\theta\cos\theta_m\sin\theta_m\cos\theta. \tag{49}$$

Furthermore, the numerator can be rewritten exactly in either of two useful forms:

$$\sin^2(\theta+\theta_m) + \sin^2(\theta-\theta_m) = [\sin(\theta_m+\theta) + \sin(\theta_m-\theta)]^2 - 2\sin(\theta_m+\theta)\sin(\theta_m-\theta) \tag{50}$$

$$= 4\sin^2\theta_m\cos^2\theta - (\cos 2\theta - \cos 2\theta_m), \tag{51}$$

or

$$\sin^2(\theta+\theta_m) + \sin^2(\theta-\theta_m) = [\sin(\theta_m+\theta) - \sin(\theta_m-\theta)]^2 + 2\sin(\theta_m+\theta)\sin(\theta_m-\theta) \tag{52}$$

$$= 4\sin^2\theta\cos\theta_m + (\cos 2\theta - \cos 2\theta_m). \tag{53}$$

Having two valid but distinct expressions [*i.e.*, (51) and (53)] for the same quantity, both expressions can be used in arbitrary weighted averages. In particular, consider multiplying (51) by $\cos^2\theta_m$ and (53) by $\sin^2\theta_m$, then the result is

$$\sin^2(\theta+\theta_m) + \sin^2(\theta-\theta_m) = 4\sin^2\theta_m\cos^2\theta_m + (\cos^2\theta_m - \sin^2\theta_m)^2$$
$$- \cos 2\theta(\cos^2\theta_m - \sin^2\theta_m),$$

which conveniently simplifies to

$$\sin^2(\theta+\theta_m) + \sin^2(\theta-\theta_m) = 1 - \cos 2\theta_m\cos 2\theta. \tag{54}$$

15

The rather simple final expression is

$$\left(\frac{\tan\theta}{\tan\theta_m} + \frac{\tan\theta_m}{\tan\theta}\right) = 2\frac{1 - \cos 2\theta_m \cos 2\theta}{\sin 2\theta_m \sin 2\theta}. \tag{55}$$

To check one limit of this expression, consider the value at $\theta = \theta_m$. Then, the numerator equals $\sin^2 2\theta_m$, and the denominator equals $\frac{1}{2}\sin^2 2\theta_m$. So the result equals 2, as it should.

APPENDIX C: HTI FORMULAS FROM VTI FORMULAS

Probably the easiest way to obtain formulas pertinent to HTI (horizontal transverse isotropy) from VTI (vertical transverse isotropy) is to leave the stiffness matrix c_{ij} alone, and simply reinterpret the meaning of the indices i, j. For VTI media, one typical choice is $x_3 = z$, where $\hat{z}$ is the vertical direction at the surface of the earth, or more often the direction down into the earth. Then, the angle of incidence θ is measured with respect to $\hat{z}$, where $\theta = 0$ means parallel to $\hat{z}$ and pointing into the earth, and $\theta = \pi/2$ means horizontal incidence.

Considering aligned vertical fractures, with their axes of symmetry in the direction $x \equiv x_3$, the matrix c_{ij} itself presented in the main text need not change, but the meaning of the angles does change. Clearly, the simplest case to study, and the only one to be analyzed here, is the case of waves propagating at some angle to vertical but always in the direction $x_3 = x$, thus lying in the xz-plane perpendicular to the fracture plane. Then,

$$\theta^H + \theta^V = \frac{\pi}{2}, \tag{56}$$

where θ^V corresponds exactly to the θ appearing in all the formulas up to Eq. (39) in the main text, and θ^H is the effective angle in the xz-plane of incidence under consideration, $i.e.$, the one perpendicular to the vertical fractures in the reservoir. To obtain wave speeds at the angle θ^H, we only need to substitute $\theta \equiv \theta^V = \frac{\pi}{2} - \theta^H$, or write the speeds as

$$^H v_p^2(\theta^H) \equiv v_p^2(\theta^V) = v_p^2(\frac{\pi}{2} - \theta^H), \tag{57}$$

$$^H v_{sv}^2(\theta^H) \equiv v_{sv}^2(\theta^V) = v_p^2(\frac{\pi}{2} - \theta^H), \tag{58}$$

and

$$^H v_{sh}^2(\theta^H) \equiv v_{sh}^2(\theta^V) = v_p^2(\frac{\pi}{2} - \theta^H). \tag{59}$$

16

Since all the angular dependence in the exact formulas is in the form of $\sin^2\theta$ and $\cos^2\theta$, and since $\sin^2(\frac{\pi}{2}-\theta) = cos^2\theta$ and vice versa, the entire procedure amounts to switching the locations of $\sin^2\theta$ and $\cos^2\theta$ with $\cos^2\theta^H$ and $\sin^2\theta^H$ everywhere in the exact expressions.

This procedure is obviously very straightforward to implement. The final results analogous to Thomsen's formulas are:

$$^Hv_p(\theta^H)/^Hv_p(0) \simeq 1 - \frac{\epsilon}{1+2\epsilon}\sin^2\theta^H - \frac{\epsilon-\delta}{1+2\epsilon}\frac{2\cos^2\theta_m^H\sin^2\theta^H\cos^2\theta^H}{[1-\cos 2\theta^H\cos 2\theta_m^H]}, \tag{60}$$

$$^Hv_{sv}(\theta^H)/^Hv_{sv}(0) \simeq 1 + [c_{33}/c_{44}]\,(\epsilon-\delta)\frac{2\cos^2\theta_m^H\sin^2\theta^H\cos^2\theta^H}{[1-\cos 2\theta^H\cos 2\theta_m^H]}. \tag{61}$$

and

$$^Hv_{sh}(\theta^H)/^Hv_{sh}(0) \simeq 1 - \frac{\gamma}{1+2\gamma}\sin^2\theta^H. \tag{62}$$

And the $\theta^H = 0$ velocities are: $^Hv_p(0) = \sqrt{c_{11}/\rho} = \sqrt{c_{33}(1+2\epsilon)/\rho}$, $^Hv_{sv}(0) \equiv \sqrt{c_{44}/\rho} = v_s(0)$, and $^Hv_{sh}(0) \equiv \sqrt{c_{66}/\rho} = \sqrt{c_{44}(1+2\gamma)/\rho}$. Also, recall that $\cos^2\theta_m^H = \sin^2\theta_m^V$.

For azimuthal angles $\phi \neq \pm\frac{\pi}{2}$, the algorithm for computing the wave speeds is to replace $\sin^2\theta^V$ by $\cos^2\theta^H\sin^2\phi$ and $\cos\theta^V = 1 - \sin^2\theta^V$ by $1 - \cos^2\theta^H\sin^2\phi$ in the exact formulas, and corresponding replacements in the approximate ones. Then, there is no angular dependence when $\phi = 0$ or π as our point of view is within the place of the fracture itself. And, when $\phi = \pm\frac{\pi}{2}$, the above stated results for the xz-plane hold.

Wave equation reciprocity guarantees that the polarizations of the various waves are of the same types as this translation from VTI media to HTI media is made.

It is also worth pointing out that the designations SH and SV for the shear waves are, however, not really valid for the HTI case. For VTI media, the quasi-SH-wave really does have horizontal polarization at least at $\theta = 0$ and $\pi/2$, whereas the corresponding wave for HTI media, instead has polarization parallel ($\parallel$) to the fracture plane. For VTI media, the so-called quasi-SV-wave has its polarization in the plane of propagation, but this polarization direction is only truly vertical for $\theta = \pm\frac{\pi}{2}$, at which point its polarization is both vertical and perpendicular to the horizontal plane of symmetry. The corresponding situation for HTI media has the wave corresponding to the SV-wave with polarization again in the plane of propagation, but this is actually only vertical at $\theta^H = \frac{\pi}{2}$, and also parallel to the fracture plane; however, for all other angles its polarization has a component that is perpendicular ($\perp$) to the plane of the fractures. So a more accurate naming convention for these waves

17

would make use of the following designations:

$$^H v_{sh}(\theta^H) \rightarrow^H v_{s\parallel}(\theta^H), \tag{63}$$

for the HTI wave corresponding to the quasi-SH-wave in the VTI case, and

$$^H v_{sv}(\theta^H) \rightarrow^H v_{s\perp}(\theta^H), \tag{64}$$

for the HTI wave corresponding to the quasi-SV-wave in the VTI case. Although this notation is hereby being recommended, it will actually not be used in the main text as the current choices and various caveats will no doubt be sufficiently familier to most readers that it may not be essential to make this change at this time. [Note that Thomsen (2002) uses the same $\parallel$ and $\perp$ notation for similar purposes.]

REFERENCES

Backus, G. E., 1962, Long-wave elastic anisotropy produced by horizontal layering: *J. Geophys. Res.*, **67**, 4427–4440.

Berryman, J. G., 1979, Long-wave elastic anisotropy in transversely isotropic media: *Geophysics*, **44**, 896–917.

Berryman, J. G., and Grechka, V., 2006, Random polycrystals of grains containing cracks: Model of quasistatic elastic behavior for fractured systems: *J. Appl. Phys.*, **100**, 113527.

Grechka, V., and Kachanov, M. 2006a, Effective elasticity of fractured rocks: *The Leading Edge*, **25**, 152–155.

Grechka, V., and Kachanov, M., 2006b, Effective elasticity of rocks with closely spaced and intersecting cracks: *Geophysics*, **71**, D85–D91.

Kachanov, M., 1980, Continuum model of medium with cracks: *ASCE J. Engineering Mech.*, **106**, 1039–1051.

Musgrave, M. J. P., 1959, The propagation of elastic waves in crystals and other anisotropic media: *Reports Prog. Phys.*, **22**, 74–96.

Musgrave, M. J. P., 2003, *Crystal Acoustics*: Acoustical Society of America, Leetsdale, Pennsylvania, Chapter 8.

Rüger, A., 2002, *Reflection Coefficients and Azimuthal AVO Analysis in Anisotropic Media*: Geophysical Monographs Series, Number 10, SEG, Tulsa, OK.

Sayers, C. M., and Kachanov, M., 1991, A simple technique for finding effective elastic constants of cracked solids for arbitrary crack orientation statistics. *Int. J. Solids Struct.*, **27**, 671–680.

Thomsen, L., 1986, Weak elastic anisotropy: *Geophysics*, **51**, 1954–1966.

Thomsen, L., 2002, *Understanding Seismic Anisotropy in Exploration and Exploitation*: 2002 Distinguished Instructor Short Course, Number 5, SEG, Tulsa, OK.

Tsvankin, I., 1997, Anisotropic parameters and *P*-wave velocity for orthorhombic media: *Geophysics*, **62**, 1292–1309.

Tsvankin, I., 2005, *Seismic Signatures and Analysis of Reflection Data in Anisotropic Media*: Handbook of Geophysical Exploration, Seismic Exploration, Volume 29, Elsevier, Amsterdam.

TABLE 1. Values of five crack-influence parameters for the two models considered.

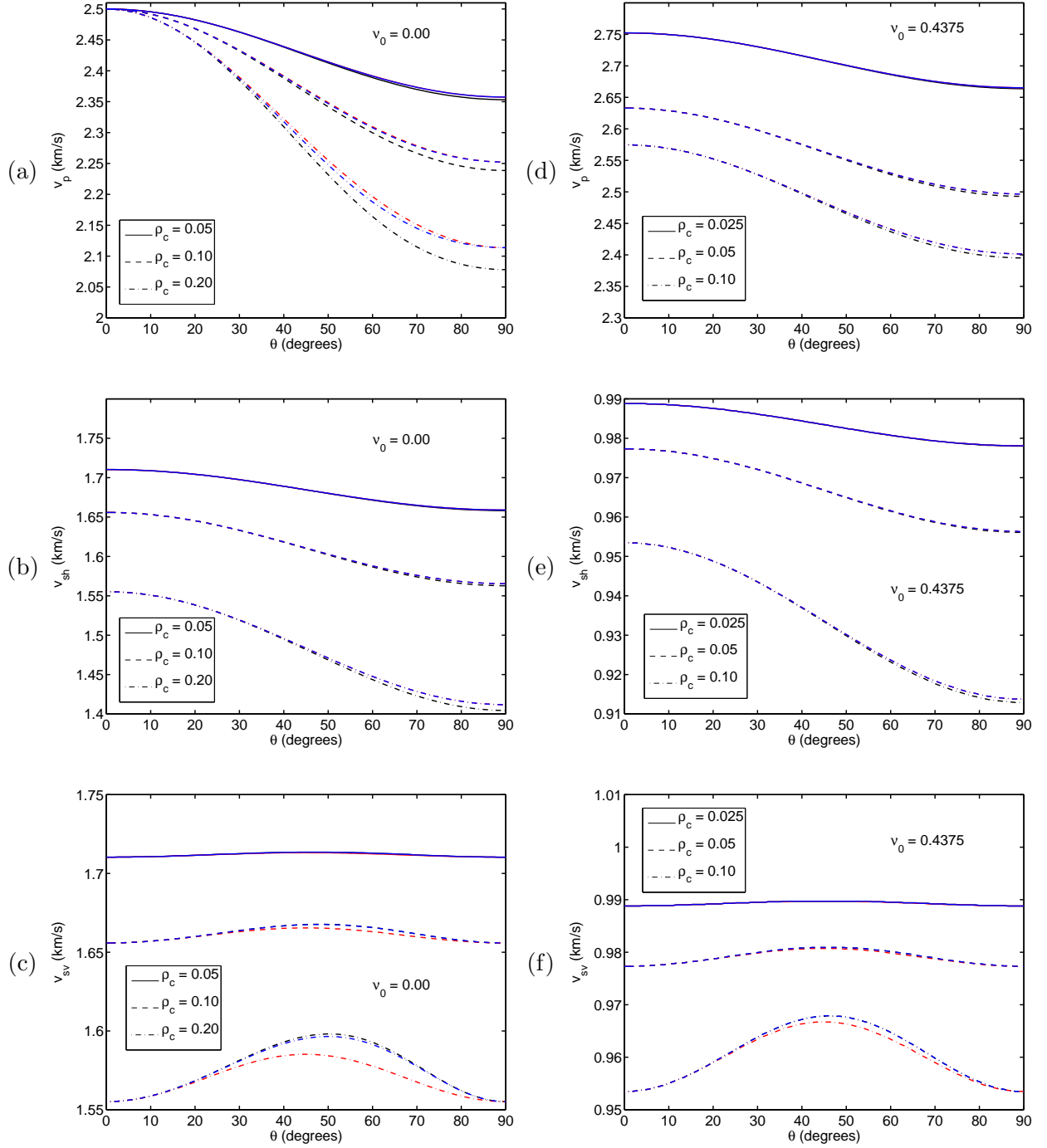| Crack-influence Parameters	First Model $\nu_0 = 0.00$	Second Model $\nu_0 = 0.4375$
$\eta_1(0)$ (GPa^{-1})	0.0000	-0.0192
$\eta_2(0)$ (GPa^{-1})	0.1941	0.3994
$\eta_3(0)$ (GPa^{-1})	-0.3666	-1.3750
$\eta_4(0)$ (GPa^{-1})	0.0000	0.0000
$\eta_5(0)$ (GPa^{-1})	0.0917	0.5500

FIG. 1: For vertical cracks and VTI symmetry: examples of anisotropic compressional wave speed (v_p), SH shear wave speed (v_{sh}), and SV shear wave speed (v_{sv}) for two values of Poisson's ratio ν_0 of the host medium: (a)–(c) $\nu_0 = 0.00$, (d)–(f) $\nu_0 = 0.4375$. Velocity curves in black are exact for the fracture model discussed in the text. The Thomsen weak anisotropy velocity curves for the same fracture model are then overlain in red. Finally, the new curves for the extended Thomsen approximation valid for stronger anisotropies are overlain in blue.
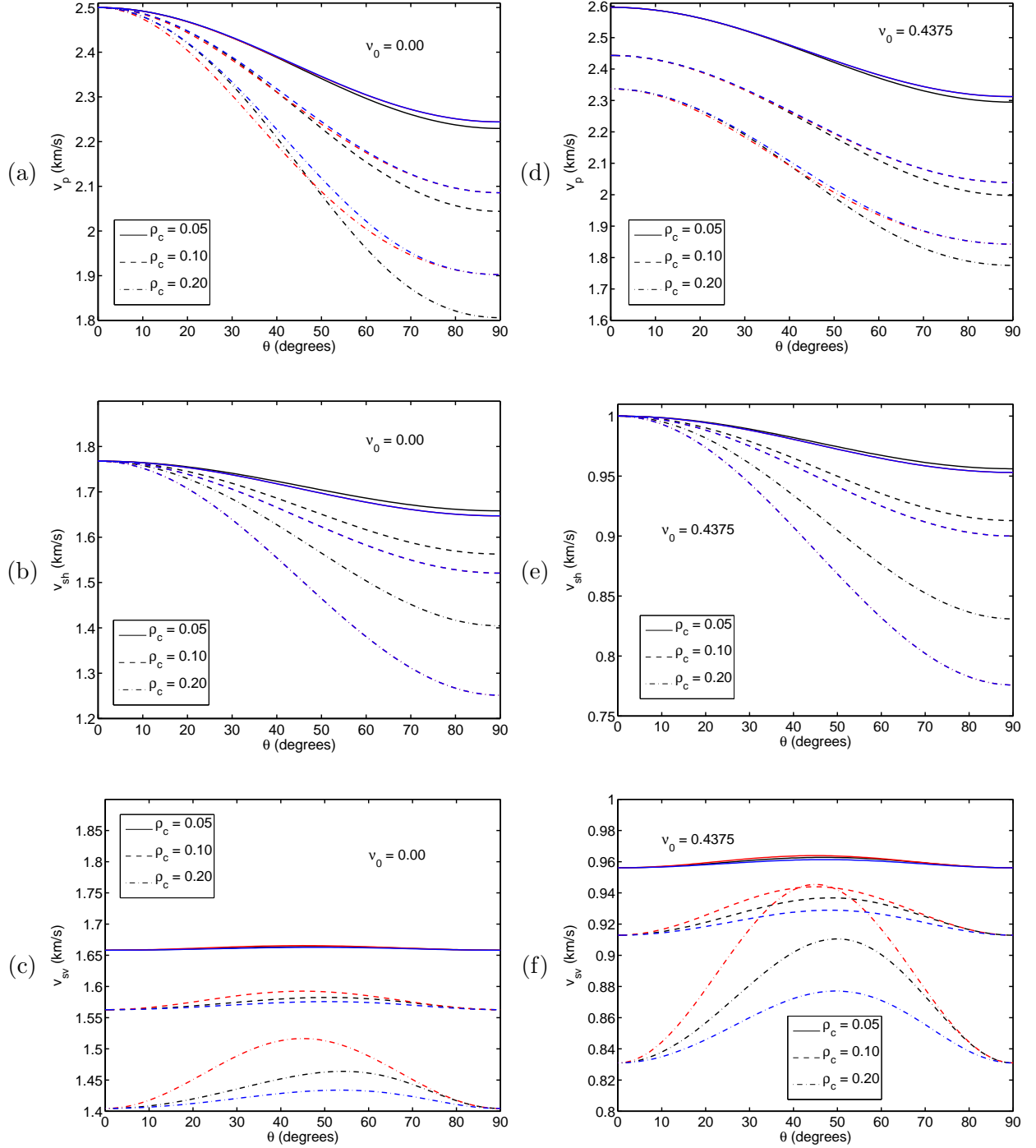
FIG. 2: For vertical cracks and HTI symmetry: examples of anisotropic compressional wave speed (v_p), SH shear wave speed (v_{sh}), and SV shear wave speed (v_{sv}) for two values of Poisson's ratio ν_0 of the host medium: (a)–(c) $\nu_0 = 0.00$, (d)–(f) $\nu_0 = 0.4375$. Velocity curves in black are exact for the fracture model discussed in the text. The Thomsen weak anisotropy velocity curves for the same fracture model are then overlain in red. Finally, the new curves for the extended Thomsen approximation valid for stronger anisotropies are overlain in blue.

22